

Effect of Sulfation of Zirconia on Catalytic Performance in the Dehydration of Aliphatic Alcohols

Ya-Sun Hsu (許雅珊), Yin-Lan Wang (王音嵐) and An-Nan Ko* (柯安男)
Department of Chemistry, Tunghai University, Taichung, Taiwan, R.O.C.

Catalytic dehydration of 2-propanol and that of 1-butanol were performed at atmospheric pressure and 150-300 °C over ZrO₂ and sulfated ZrO₂ (S/ZrO₂) in a fixed-bed, tubular reactor. The catalysts were characterized with XRD, elemental analysis, FT-IR, N₂ physisorption, TG/DTA, TPD, and TPR. The main structures of ZrO₂ and S/ZrO₂ were monoclinic and tetragonal, respectively. As ZrO₂ was modified with sulfuric acid, its surface area and acid amount were greatly increased, whereas the pore volume, the pore diameter, and the particle size were reduced. Both samples owned weak basicity. For both reactions, only dehydration products of alkene and ether were obtained. The alcohol conversion enhanced remarkably with the catalyst acid amount and the surface area as well as the reaction temperature. In addition, the ether selectivity on S/ZrO₂ decreased with raising the reaction temperature. The activation energy was 81.0 kJ/mol in the propene formation from 2-propanol over S/ZrO₂. The corresponding value was 94.4 kJ/mol for the dehydration of 1-butanol.

Keywords: Zirconia; Sulfated zirconia; Dehydration; Catalyst characterization; 2-Propanol; 1-Butanol.

INTRODUCTION

Solid acid catalysis has drawn much attention due to its great potential for both academic research and industrial applications.¹ Up to now, zirconia has been intensively studied for its utilization as a solid support and a catalyst since it exhibits acidic, basic, oxidizing and reducing surface properties.^{2,3} Zirconia possesses three different crystalline structures, viz monoclinic, tetragonal and cubic phase, depending on the treatment conditions.⁴ After modification with sulfate anions, the sulfated zirconia mainly has a tetragonal structure at high calcined temperature.⁵

According to the results obtained from various techniques such as IR, Raman spectroscopy, XPS, thermal analysis and XRD, many models were proposed to describe the formation mechanism and the structure of sulfated zirconia.⁶⁻¹⁰ Despite much efforts were done on the characterization of physical properties of sulfated zirconia, the exact structure and the nature of acid sites still remain a subject of large debate. However, it is widely accepted that the adsorption of sulfate anions on the zirconia surface generates highly acidic or superacidic properties. Consequently, this material has been utilized to catalyze a variety of reactions such as isomerization, dehydration, alkylation, acylation, esterification, condensation, nitration, cyclization, etc. as reported in the review papers.^{11,12}

The catalytic conversion of aliphatic alcohols has been carried out using a variety of catalysts possessing acidic and/or basic sites, i.e., metal oxides, mixed metal oxides, clays, pillared clays and molecular sieves.^{4,13-16} Pure zirconia, sulfated zirconia, zirconia based binary and ternary oxides were prepared and applied to the reactions of ethanol,¹⁷ 2-propanol,¹⁸⁻²² 2-butanol,²³ 4-methyl-pentan-2-ol,²⁴ and 2-octanol.²⁵ Among these alcohols studied, the conversion of 2-propanol was often used as a model reaction to probe catalyst acid-base properties. For this reaction over TiO₂, ZrO₂ and CeO₂ at 473-623 K, higher activity and acetone selectivity were observed in flowing air than in helium or hydrogen.¹⁸ Sulfated ZrO₂-TiO₂ containing Ti mole fraction 0.4 possessed the largest amount of sulfur, the highest acidity and also the best activity.¹⁹ A new solid superacid catalyst was prepared by doping sulfated ZrO₂ with Ce that greatly enhanced the surface area and stabilized the tetragonal phase. The catalytic activity was in line with the catalyst acidity.²² The dehydration of 2-butanol over a sulfated zirconia/ γ -alumina catalyst was performed in the injection port of a gas chromatograph. The kinetics were found to be a pseudo-first-order reaction mechanism.²³

Recently the dehydration of 1-butanol has attracted increasing interest using various solid catalysts, viz sil-

ica-alumina,²⁶ AlPO₄ and modified AlPO₄,^{27,28} pillared clays²⁹⁻³¹ and nitrated aluminophosphate.³² The acidity-basicity of silica-alumina depended on the alumina content which affected the catalytic activity and product selectivity.²⁶ Modification of AlPO₄ with SO₄²⁻ ions caused an increase of the number of strong acid sites, whereas opposite trend occurred with Na⁺ ions. The butenes selectivity enhanced with the catalyst strong acidity.²⁷ With phosphorus-modified aluminum pillared montmorillonite, the 1-butanol conversion was well associated with Lewis acidity.²⁹ So far, to the best of our knowledge no report has been found for the 1-butanol dehydration over sulfated zirconia catalysts. In this study, zirconia and sulfated zirconia were prepared. Both catalysts were characterized with various techniques to determine their physico-chemical properties. The reaction of 2-propanol and that of 1-butanol were utilized as test reactions to compare the catalytic performance among these catalysts. The kinetic parameters for both reactions were estimated; the apparent rate constants were correlated with the catalyst properties.

EXPERIMENTAL SECTION

Catalyst preparation

Zirconium oxide was prepared by dissolving 25 g of zirconyl (IV) chloride octahydrate (ZrOCl₂·8H₂O, Acros) in 200 mL de-ionized water. The solution was stirred at 98 °C for 2 h into which was added dropwise aqueous ammonia solution until a pH value of 9.3 with subsequent filtration and washing to obtain Zr(OH)₄. This compound was dried at 100 °C for 24 h, heated at 1 °C/min up to 600 °C and calcined for 3 h to produce ZrO₂.

To prepare sulfated ZrO₂, 1 g of Zr(OH)₄ was mixed with 15 mL of 1 M sulfuric acid and stirred for 0.5 h. After filtration, the sample was dried at 100 °C for 24 h, heated at 1 °C/min to 600 °C and calcined for 3 h to form sulfated ZrO₂ (S/ZrO₂).

Catalyst characterization

The content of sulfur in S/ZrO₂ was measured with an elemental analyzer (elementar vario EL III) and was found to be 2.3 wt.%.

The powder X-ray diffraction patterns of various samples were recorded using a Shimadzu XRD-6000 diffractometer with Ni filtered CuK α radiation ($\lambda = 0.154$ nm) in the range of $2\theta = 20-70^\circ$ at a scanning speed of $2^\circ/\text{min}$. The mean particle sizes D (nm) of ZrO₂ and S/ZrO₂ were calculated from the (111) reflex of the monoclinic form at $2\theta = 28.19^\circ$ and that of tetragonal form at $2\theta = 30.63^\circ$, re-

spectively, according to the Debye-Scherrer equation.

$$D = K\lambda/\beta\cos\theta$$

where K is the crystallite shape constant (~ 1), λ is the X-ray wavelength (nm), β is the width of half height peak (radian), and θ is the Bragg angle (degree).

The N₂ physisorption was conducted at 77 K with a Micromeritics system ASAP 2020 to obtain the specific surface area, the N₂ adsorption/desorption isotherm, the pore volume, and the pore size distribution. Prior to each run, the sample was pre-treated at 110 ° under a pressure of 1×10^{-4} torr for 2 h.

FT-IR spectra of ZrO₂ and S/ZrO₂ samples were taken for the pellets of these samples mixed with KBr at room temperature in the transmission mode with resolution of 2 cm^{-1} by a Perkin-Elmer system 2000 spectrometer.

The TG/DTA analysis was performed with an EXSTAR 6000 series instrument. A 0.01 g of sample was heated in the air (20 °C/min) from 50 to 900 °C. The weight loss and heat flow were measured as a function of temperature.

The catalyst acidity and basicity were determined by a self-designed temperature programmed desorption (TPD) apparatus, containing a quartz reactor (i.d. = 4 mm) and a T.C.D. detector. In a typical run, 0.1 g of catalyst was heated up to 500 °C under helium flow (40 mL/min) with a rate of 10 °C/min and then cooled to room temperature. Then several pulses of ammonia or carbon dioxide were injected into the reactor until saturated adsorption. The temperature was increased to 100 °C and kept there for 2 h to remove the physisorbed ammonia. Finally the system was heated from 110 to 600 °C at a rate of 10 °C/min and the desorbed gas was monitored with a T.C.D. detector.

For the analysis of temperature programmed reduction (TPR) the same apparatus as that of TPD was utilized. A gaseous mixture of hydrogen and argon (1:10) with a flow rate of 30 mL/min passed through the reactor at 110 °C for 0.5 h and then the temperature was raised to 750 °C at a rate of 10 °C/min.

Catalytic reaction

The catalytic dehydration of 2-propanol and that of 1-butanol were performed at atmospheric pressure and 150-300 °C in a fixed-bed, integral flow reactor (2 cm i.d. \times 49 cm) with down flow mode. The reactor was placed in a vertical furnace and the catalyst sample (0.02-0.5 g) diluted with glass particles of similar sizes was loaded in the middle part of the reactor. A thermocouple was situated

near the catalyst in order to measure the reaction temperature. Prior to the reaction, the catalyst was activated at 400 °C with flowing air (60 mL/min) for 1 h to remove water vapor and carbon dioxide, followed by cooling to the reaction temperature with flowing N₂ gas (60 mL/min). Then the reactant was fed into the reactor via a microfeeder (Stoelting). The unconverted alcohol and the products were condensed, collected periodically and analyzed by a HP 5890 gas chromatograph fitted with a FFAP capillary column (50 m × 0.2 mm) and a flame-ionization detector.

RESULTS AND DISCUSSION

XRD results

The dependence of ZrO₂ crystalline structure on the calcination temperature was studied previously; ZrO₂ was amorphous up to 300 °C, tetragonal phase at 350 °C, a mixture of tetragonal and monoclinic form at 400–800 °C and a pure monoclinic phase at 900 °C.²² Fig. 1 displays the XRD patterns of Zr(OH)₄, ZrO₂, and S/ZrO₂. The Zr(OH)₄ sample belongs to an amorphous solid whereas ZrO₂ and S/ZrO₂ reveal well crystalline structure. In addition, ZrO₂, being calcined at 600 °C, contains mainly the monoclinic phase and partly the tetragonal phase. The peaks of monoclinic phase appear at 2θ = 24.0, 28.2, 31.5, 49.3, and 50.1°. After modification with sulfuric acid, the monoclinic phase transforms to the tetragonal phase at 2θ = 30.6, 34.0, 35.2, 49.5, and 60.1° in the sample of S/ZrO₂ that is

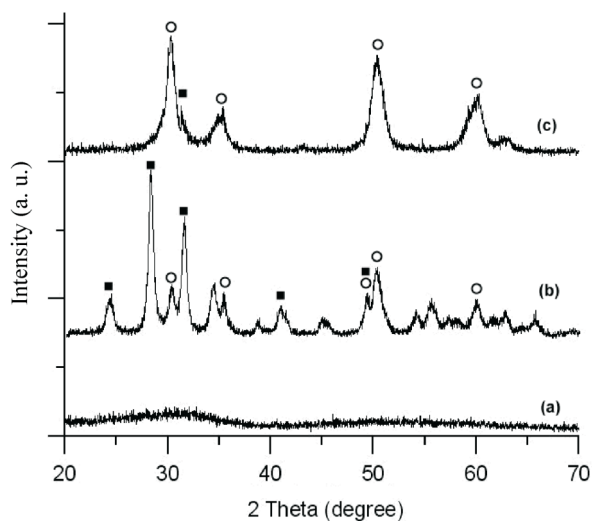


Fig. 1. Powder XRD patterns of various samples: (a) Zr(OH)₄; (b) ZrO₂; (c) S/ZrO₂; (■) monoclinic phase of ZrO₂; (○) tetragonal phase of ZrO₂.

consistent with other studies.^{17,33,34} Based on the Debye-Scherrer formula, the calculated mean particle sizes are 12.4 and 9.5 nm for ZrO₂ and S/ZrO₂, respectively. Consequently, the size of ZrO₂ particles is reduced after sulfation of ZrO₂ due to phase transformation and suppression of particle aggregation. Similar results were reported elsewhere.^{21,24,35}

Textural properties

The N₂ adsorption-desorption isotherm and the pore size distribution of various catalysts are illustrated in Fig. 2. The ZrO₂ sample exhibits a type IV isotherm, indicating the monolayer adsorption at low relative pressure (P/P₀). The degree of adsorption enhanced greatly with an hysteresis loop occurring at P/P₀ in the range of 0.7–0.9, which implies capillary condensation in the mesopores. For the S/ZrO₂ sample the adsorption also belongs to the type IV isotherm and the hysteresis loop appears at P/P₀ > 0.4.³⁶

Based on the BJH method, the calculated average pore diameters are 12.2 and 3.3 nm for ZrO₂ and S/ZrO₂, respectively. Table 1 lists the textural properties of these

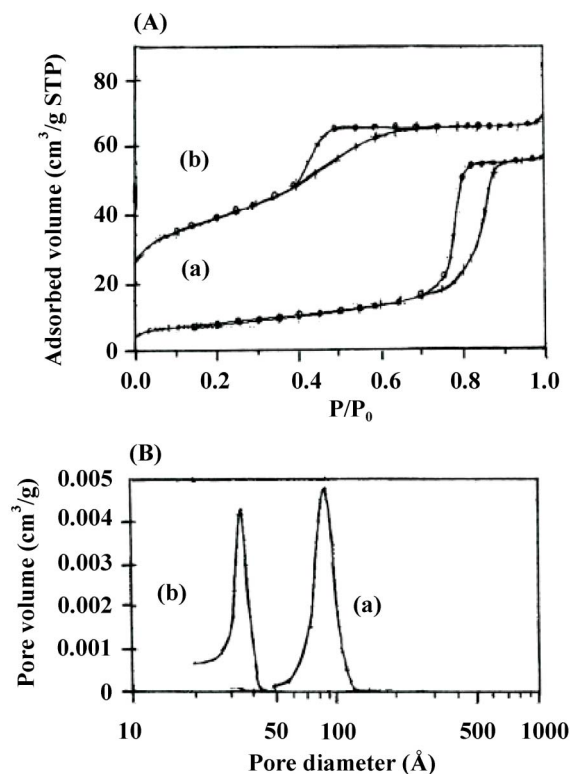


Fig. 2. N₂ physisorption: (A) adsorption-desorption isotherms; (B) pore size distribution. (a) ZrO₂; (b) S/ZrO₂.

Table 1. The physico-chemical properties of various catalysts

Catalyst	ZrO ₂	S/ZrO ₂
Sulfur content (%)	---	2.3
Surface area (m ² /g)	42.3	132
Pore diameter (nm)	12.2	3.3
Pore volume (cm ³ /g)	0.13	0.12
Particle size (nm)	12.4	9.5
Acid amount (mmol/g)	0.21	0.40
Base amount (mmol/g)	0.056	0.042

two samples. Sulfation of ZrO₂ causes an enormous increase of the surface area with concomitant decrease of pore diameter, pore volume and particle size. These results are comparable to the literature reports.^{22,33,35}

FT-IR study

Fig. 3 illustrates the FT-IR spectra of ZrO₂ and S/ZrO₂. With ZrO₂, the band at 1625 cm⁻¹ is ascribed to the bending vibration mode of the adsorbed water while that at 1550 cm⁻¹ is assigned to the -OH vibration mode.³⁷ After modification of ZrO₂ with sulfuric acid, the band at 998 cm⁻¹ is assigned to the S-O symmetric stretching ν_1 whereas those bands of 1027, 1073, 1138, and 1228 cm⁻¹ are attributed to the splitting of the S-O asymmetric stretching ν_3 , which implies the existence of sulfate species as bidentate complexes coordinated to ZrO₂.^{21,38} Sohn et al.²¹ observed a sharp band at 1364-1390 cm⁻¹ in the FT-IR spectra of self-

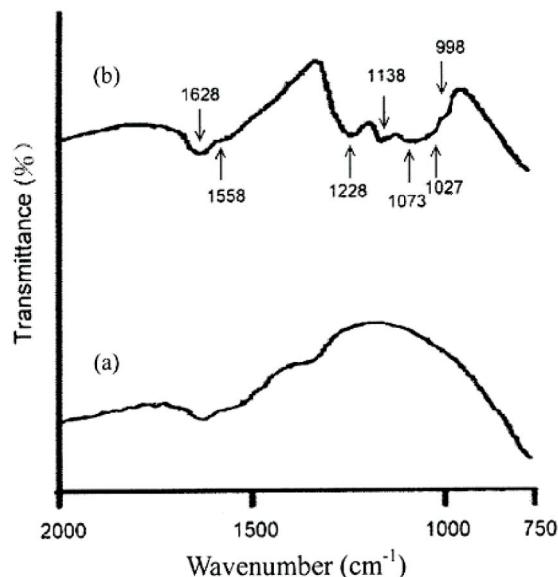


Fig. 3. FT-IR spectra of various samples: (a) ZrO₂; (b) S/ZrO₂.

supported 3Ce-ZrO₂/SO₄²⁻ after evacuation (≥ 200 °C) for 1 h, which indicates the asymmetric S=O stretching frequency of sulfate ion bonded to ZrO₂. However, this band was not detected in this study because the S/ZrO₂ sample was not evacuated prior to FT-IR measurements and water molecules were adsorbed on the surface.^{4,6}

Thermal analysis

Fig. 4 depicts TG/DTA curves for various samples predried at 110 °C. The weight losses below 250 °C are 0.85 and 2.46%, for ZrO₂ and S/ZrO₂, respectively, which are attributed to the evolution of water vapor. The weight losses between 610 and 660 °C are very small for both samples while the losses above 660 °C are negligible and 2.7%, indicating the slight decomposition of sulfate group in the S/ZrO₂ sample.

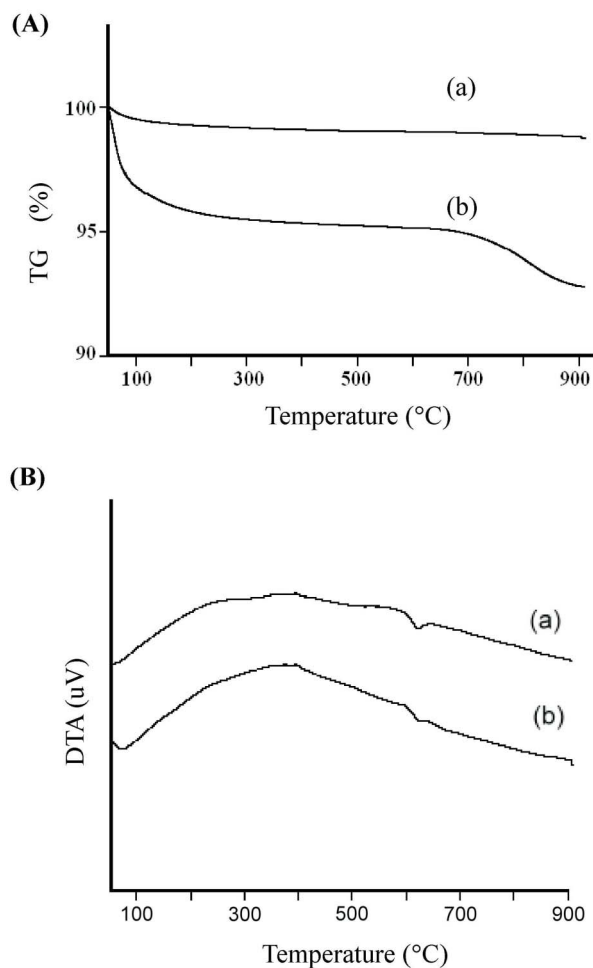


Fig. 4. Thermal analysis patterns: (A) TG curves; (B) DTA curves. (a) ZrO₂; (b) S/ZrO₂.

The DTA curves of the two samples show endothermic peaks below 250 °C, implying the removal of physisorbed water. In addition, small peaks around 630 °C are observed due to a small extent of phase transition from tetragonal to monoclinic form since it corresponds to a constant weight region in the TG results.

TPD results

The catalyst acidity and basicity can be determined with TPD of ammonia and carbon dioxide, respectively. Fig. 5 shows the TPD of ammonia profiles from various samples. For ZrO₂, the curve reveals a small and broad peak. The S/ZrO₂ sample exhibits a much larger peak, which rises remarkably to a maximum at ~200 °C and thereafter declines. All samples exhibit a small shoulder peak at 600 °C exactly when the heating program was switched off. This is possibly due to the effect of increasing then decreasing temperature because a TCD detector was used in monitoring desorbed ammonia.³⁹ The acid amount was estimated from the peak area of TPD plots in association with calibration data. In this way, both the acid amount and acid strength follow the order of S/ZrO₂ >> ZrO₂. It was pointed out that the acid sites are correlated to the Zr⁴⁺ cation and the acid strength is enhanced due to several factors such as the induction effect of S=O group in the sulfate species as well as the valency, the electronegativity, and coordination number of Zr⁴⁺ cation.²² According to the TPD plots of carbon dioxide (not shown), both catalysts possess quite low basicity. The data are listed in Table 1.

TPR analysis

The catalyst reduction behavior was determined by the TPR technique. The TPR profiles are displayed in Fig.

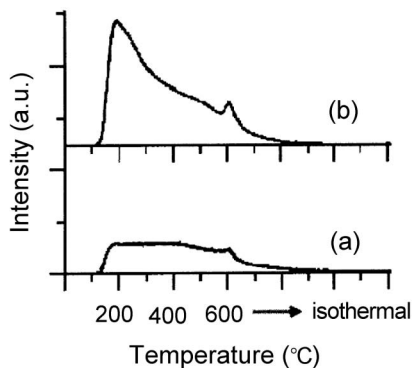


Fig. 5. Ammonia TPD profiles for various samples: (a) ZrO₂; (b) S/ZrO₂.

6. For pure ZrO₂ two relatively small H₂ uptake signals are observed at 460 and 610 °C in fair agreement with the literature,³⁴ in which the former one was proposed to arise from elimination of lattice oxygen, leading to the formation of anionic vacancies while the latter one was associated with the bulk reduction or hydride production. In the case of S/ZrO₂ only one peak appears at high temperature of 710 °C. As no corresponding peak is found for pure ZrO₂, this peak is assigned to the reduction of sulfate species as reported by other investigators.^{40,41} According to the above results and those of XRD, TG/DTA, and TPR studies, it is noteworthy that sulfation of ZrO₂ causes the stabilization of tetragonal structure as well as the resistance of ZrO₂ reduction with H₂ gas.

2-Propanol dehydration

So far, the catalytic conversion of aliphatic alcohols has attracted considerable interest. The dehydration products, olefins and ethers, are formed on acid sites, whereas the dehydrogenation products, aldehydes or ketones, are produced via both acid and base sites. Consequently, the dehydration rate enhances with the catalyst acidity while the ratio of the dehydrogenation rate to the dehydration rate is parallel to the catalyst basicity.^{1,42} In this study the dehydration products include propene and diisopropyl ether (DIPE), which are formed on the acid sites. Similar results were reported for this reaction over a variety of catalysts.^{15,16,20} Propene is produced via intramolecular E1 mechanism, whereas DIPE is obtained by intermolecular

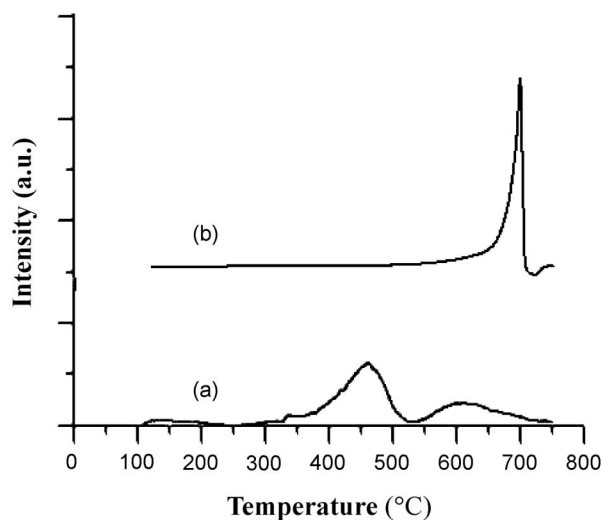


Fig. 6. H₂ TPR profiles for various samples: (a) ZrO₂; (b) S/ZrO₂.

Table 2. Catalytic results of 2-propanol. W/F, 0.008 h; Time-on-stream, 30 min

Catalyst	Temperature (°C)	Conversion (mol%)	Selectivity (mol%) ^a	
			Propene	DIPE
ZrO ₂	250	0.58	100	0
S/ZrO ₂	150	21.5	69.3	30.7
	165	27.6	71.5	28.5
	180	48.4	82.0	18.0
	200	78.6	98.0	2.0

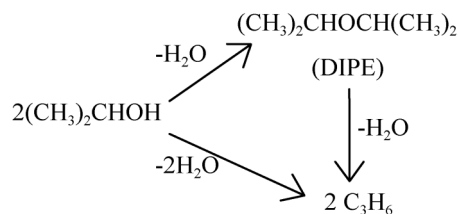
^a DIPE, diisopropylether

substitution reaction. No acetone is produced for all reaction runs since these catalysts own weak basicity.

The 2-propanol conversion and the product selectivity are calculated on the basis of converted 2-propanol. Table 2 summaries the results of 2-propanol dehydration over pure zirconia and sulfated zirconia. In the temperature range between 150 and 200 °C, ZrO₂ exhibits no catalytic activity, whereas S/ZrO₂ shows drastically higher activity. The remarkable activity difference among the two catalysts is attributed to their relative acid amount and surface area as well as crystalline structure. As mentioned earlier, sulfation of zirconia induces the structural stabilization of tetragonal phase, which is known to associate with the catalyst activity. Moreover, such a process enhances the catalyst acid amount and retards the particle aggregation, leading to smaller particle size and larger surface area (Table 1). All these factors result in the activity trend of S/ZrO₂ ≫ ZrO₂.

The space time W/F is the ratio of catalyst weight (g) to the feed rate (g/h). Fig. 7 shows the evolution of propene to DIPE molar ratio as a function of the space time at 180 °C. The initial molar ratios is 3.2 over S/ZrO₂ obtained by extrapolating to zero value of W/F; it refers to the initial selectivity ratios of propene to DIPE. The fact that this ratio increases with increasing the space time implies propene to be a primary and secondary product. The reaction network (Scheme I) is thus shown as follows:

Scheme I



The above reaction pathway is a combination of parallel and consecutive reactions in accordance with other reports.^{13,16} As revealed in Table 1, increasing temperature enhances the catalytic activity. In addition, a rise of temperature favors the propene selectivity, which is attributed to reduction of DIPE formation caused by further reaction of DIPE to propene.

The DIPE selectivity in many runs is not small enough to be neglected under our operating conditions. To simplify the kinetic analysis, only the kinetic parameters for the initial conversion of 2-propanol to form propene are calculated. It is known that this reaction follows the first order kinetics.^{43,44} Accordingly, the following equation is utilized:

$$dx_p/d(W/F) \big|_{W/F \rightarrow 0} = k_p$$

The symbols x_p and k_p refer to the mole percentage of propene and the apparent rate constant, respectively. k_p is the slope of the tangent line to the curve in the plot of x_p versus W/F. Hence the rate constant k_p is obtained at zero space time. With S/ZrO₂, the values of k_p are 33.4, 83.1, 200, and 369 h⁻¹ at 150, 165, 180, and 200 °C, respectively. Fig. 8 shows the Arrhenius plots for the conversion of 2-propanol to propene. The activation energy (E_a) and Arrhenius frequency factor (A) are 81.0 kJ/mol and 3.60×10^{11} h⁻¹ for 2-propene formation on S/ZrO₂. For the sake of comparison, the activation energies in the literature were reported to be 30.66-177.66 kJ/mol on ZrO₂-TiO₂ catalysts,⁴⁵ 139.5 kJ/mol on LaY zeolite,¹⁴ and 31.33-32.89 kJ/mol on 8-10 wt.% sulfuric acid modified TiO₂-SiO₂,⁴⁶ 76.74 and 89.28 kJ/mol on chromia and alumina pillared montmorillonite pillared at 500 °C, respectively.⁴⁴

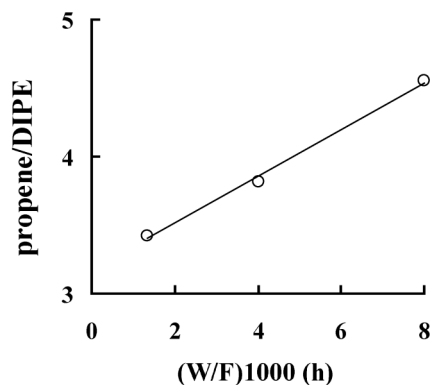
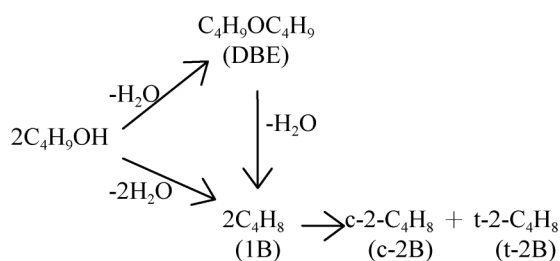


Fig. 7. The propene/DIPE molar ratio as a function of the space time over S/ZrO₂ at 180 °C.

1-Butanol dehydration

The conversion of 1-butanol was performed at atmospheric pressure and in the temperature range of 150–300 °C. The products are 1-butene (1B), *cis*- and *trans*-2-butene (*c*- & *t*-2B), and dibutylether (DBE). No aldehyde or ketone was detected. 1B is formed via intramolecular dehydration while DBE is produced by intermolecular substitution reaction. *c*- and *t*-2B are secondary products, formed by isomerization of 1B. As reported previously,³² the following Scheme II illustrates the reaction network.

Scheme II



The 1-butanol conversion and the product selectivity are calculated with respect to converted 1-butanol. Table 3 presents catalytic results at 0.031 h space time and 30 min time-on-stream. Pure zirconia exhibits little activity even at the highest temperature of 300 °C. In contrast, S/ZrO₂ possesses much higher activities, which follows the same trend as that in 2-propanol reaction. The activity difference is in line with the catalyst acidity and surface area. A comparison between 2-propanol and 1-butanol conversion clearly reveals that, as expected, the secondary alcohol of 2-propanol exhibits much higher activity (Table 2 & 3).

It is apparent that increasing temperature enhances

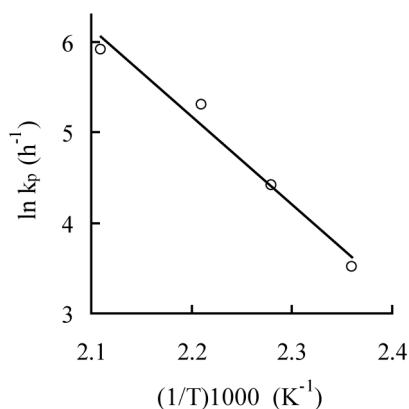


Fig. 8. Arrhenius plot for the formation of propene from 2-propanol over S/ZrO₂.

remarkably the catalytic activity. However, the effect of temperature on the product selectivity is not pronounced. The DBE selectivity diminishes slightly with a rise of temperature, whereas the *t*-2B selectivity reveals the opposite trend. Different mechanisms (E1, E2 or E1cB) were proposed to explain the product distribution of 1B, *c*- and *t*-2B in the 1-butanol dehydration.³² For this reaction over strong acidic catalysts, the intramolecular dehydration yields 1B through an E1 mechanism and then 1B isomerizes quickly to give the major products of 2B isomers with *c*-2B to *t*-2B molar ratio being close to 1. In the case of amphoteric or basic catalysts, the intramolecular dehydration occurs via an E2 or E1cB mechanism and 1B is the main product. In the present work, the product distribution from 1-butanol conversion (Table 3) clearly demonstrates that 1B was formed on the strong acid catalysts of S/ZrO₂ through E1 mechanism.

Under our reaction conditions, DBE is the minor product with its selectivity smaller than 10 mol% for most of the reaction runs. Consequently, for the kinetic analysis the conversion of 1-butanol is treated solely as the formation of 1B and 2B isomers by neglecting DBE. Therefore, the first order kinetics is applied to this reaction and the following equation is derived.

$$-\ln(1-x) = k(W/F)$$

where *x* and *k* refer to the 1-butanol conversion and the apparent rate constant, respectively. The symbols *W* and *F* represent the catalyst weight (g) and the feed rate (g/h), respectively. Fig. 9 shows the plots of $-\ln(1-x)$ as a function

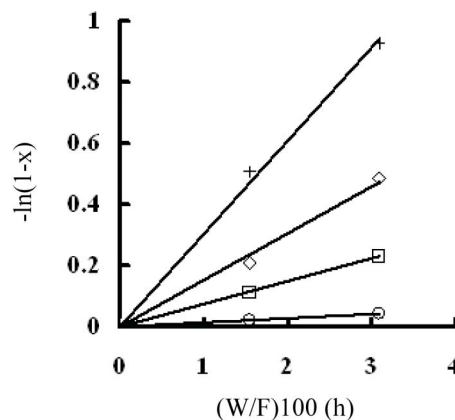


Fig. 9. Plots of $-\ln(1-x)$ versus *W/F* for 1-butanol dehydration over S/ZrO₂. (o) 150 °C; (□) 165 °C; (◇) 180 °C; (+) 200 °C.

Table 3. Catalytic results of 1-butanol dehydration. W/F, 0.031 h; Time-on-stream, 30 min

Catalyst	Temperature (°C)	Conversion (mol%)	Selectivity (mol%) ^a				c-2B	
			1B	c-2B	t-2B	DBE	t-2B	
ZrO ₂	300	0.91	71.1	16.9	12.0	0	1.41	
S/ZrO ₂	150	4.20	22.5	29.3	33.8	14.4	0.87	
	165	21.5	21.3	31.0	33.9	13.8	0.92	
	180	37.8	20.7	31.1	38.7	9.5	0.80	
	200	59.8	18.3	31.1	45.1	5.5	0.69	

^a 1B, 1-butene; t-2B, t-2-butene; c-2B, c-2-butene; DBE, dibutylether

of the space time W/F over S/ZrO₂. Straight lines passing through the origin verify that this reaction is first order and their slopes equal the rate constant k. The values of k for this reaction on S/ZrO₂ are 1.63, 7.55, 14.5, and 30.3 h⁻¹ at 150, 165, 180, and 200 °C, respectively. Fig. 10 shows the Arrhenius plots for the dehydration of 1-butanol. The values of E_a and A are 94.4 kJ/mol and 9.60 × 10¹¹ h⁻¹, respectively. The reported activation energies were 93.2 and 96.6 kJ/mol on HZSM-5 and amorphous aluminosilicate, respectively.⁴⁷ With 2-butanol dehydration over the S/ZrO₂/γ-Al₂O₃ catalyst, two activation energies were reported, i.e., 15 kJ/mol for the high temperature range (~150-325 °C) and 46 kJ/mol for the lower temperature range (75 to ~150 °C).²³

CONCLUSION

The physico-chemical properties of sulfated zirconia depend on the source and the amount of sulfate ion as well as the preparation condition. In this work, sulfation of ZrO₂ induces remarkable increase of the catalyst surface area and acid amount with concomitant decrease of the pore volume, the pore diameter, and the particle size. Both ZrO₂ and

S/ZrO₂ possess weak basicity. In addition sulfated zirconia calcined at 600 °C mainly exhibits the crystalline structure of tetragonal phase, which favors the catalytic conversion. In the reaction of 2-propanol and that of 1-butanol, the catalytic activity and the product selectivity are affected by the nature of alcohols, the catalyst property, and the reaction condition. 2-Propanol shows much higher activity than 1-butanol. With both alcohols, the conversion enhances with increasing the catalyst acidity and surface area as well as the reaction temperature. In addition, propene and 1-butene are formed on the catalyst acid sites via E1 elimination and the alkene selectivities increase with an increase of reaction temperature.

ACKNOWLEDGEMENTS

We would like to express our gratitude to the National Science Council of the Republic of China for financial support.

Received October 22, 2008.

REFERENCES

1. Tanabe, K.; Misono, M.; Ono, Y.; Hattori, H. In *New Solid Acids and Bases. Their Catalytic Properties*; Delmon, B.; Yates, J. T. Eds.; Elsevier: Amsterdam, 1989; Vol. 51.
2. Mercera, P. D. L.; Van Ommen, J. G.; Doesburg, E. B. M.; Burggraaf, A. J. *Appl. Catal.* **1990**, *57*, 127.
3. Tanabe, K. *Mat. Chem. Phys.* **1985**, *13*, 347.
4. Larsen, G.; Lotero, E.; Petkovic, L. M.; Shobe, D. S. *J. Catal.* **1997**, *169*, 67.
5. Comelli, R. A.; Vera, C. R.; Parera, J. M. *J. Catal.* **1995**, *151*, 96.
6. Yamaguchi, T. *Appl. Catal.* **1990**, *61*, 1.
7. Arata, K.; Hino, M. *Appl. Catal.* **1990**, *59*, 197.
8. Davis, B. H.; Keogh, R. A.; Srinivasan, R. *Catal. Today* **1994**, *20*, 219.
9. Clearfield, A.; Serrete, G. P. D.; Khazi-Syed, A. H. *Catal. Today* **1994**, *20*, 295.

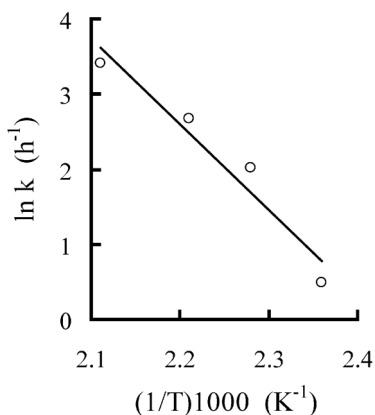


Fig. 10. Arrhenius plot for 1-butanol dehydration over S/ZrO₂.

10. Kustov, L. M.; Kazansky, V. B.; Figueras, F.; Tichit, D. *J. Catal.* **1994**, *150*, 143.
11. Song, X.; Sayari, A. *Catal. Rev. Sci. Eng.* **1996**, *38*, 329.
12. Yadav, G. D.; Nair, J. J. *Micro. Meso. Mater.* **1999**, *33*, 1.
13. Campelo, J. M.; Garcia, A.; Herencia, J. F.; Luna, D.; Marin, J. M.; Romero, A. A. *J. Catal.* **1995**, *151*, 307.
14. Rudham, R.; Spiers, A. I. *J. Chem. Soc. Faraday Trans.* **1997**, *93*, 1445.
15. Mostafa, M. R.; Youssef, A. M. *Mater. Lett.* **1998**, *34*, 405.
16. Lin, H.-E.; Ko, A.-N. *J. Chin. Chem. Soc.* **2000**, *47*, 509.
17. Ahmed, A. I.; El-Hakam, S. A.; Samra, S. E.; EL-Khouly, A. A.; Khder, A. S. *Colloids Surf., A* **2008**, *317*, 62.
18. Haffad, D.; Chambellan, A.; Lavalley, J. C. *J. Mol. Catal. A* **2001**, *168*, 153.
19. Das, D.; Mishra, H. K.; Parida, K. M.; Dalai, A. K. *J. Mol. Catal. A* **2002**, *189*, 271.
20. Manriquez, M. E.; López, T.; Gómez, R.; Navarrete, J. *J. Mol. Catal. A* **2004**, *220*, 229.
21. Sohn, J. R.; Lee, S. H.; Lim, J. S. *Catal. Today* **2006**, *116*, 143.
22. Mekhemer, G. A. H. *Colloids Surf., A* **2006**, *274*, 211.
23. Skrdla, P. J.; Lindemann, C. *Appl. Catal. A* **2003**, *246*, 227.
24. Solinas, V.; Rombi, E.; Ferino, I.; Cutrufello, M. G.; Colón, G.; Navío, J. A. *J. Mol. Catal. A* **2003**, *204-205*, 629.
25. Chokkaram, S.; Davis, B. H. *J. Mol. Catal. A* **1997**, *118*, 89.
26. Berteau, P.; Delmon, B.; Dallons, J. L.; Vangysel, A. *Appl. Catal.* **1991**, *70*, 307.
27. Bautista, F. M.; Delmon, B. *Appl. Catal. A* **1995**, *130*, 47.
28. El-Sharkawy, E. A.; Al-Shihry, S. S.; Ahmed, A. L. *Adsorp. Sci. & Tech.* **2003**, *21*, 863.
29. Shen, Y. F.; Ko, A.-N.; Grange, P. *Appl. Catal.* **1990**, *67*, 93.
30. Pires, J.; Carvalho, A. P.; Pereira, P. R.; de Carvalho, M. B. *React. Kinet. Catal. Lett.* **1998**, *65*, 9.
31. Macias, O.; Largo, J.; Pesquera, C.; Blanco, C.; Gonzalez, F. *Appl. Catal. A* **2006**, *314*, 23.
32. Delsarte, S.; Grange, P. *Appl. Catal. A* **2004**, *259*, 269.
33. Reddy, B. M.; Patil, M. K.; Rao, K. N.; Reddy, G. K. *J. Mol. Catal. A* **2006**, *258*, 302.
34. Vera, C. R.; Pieck, C. L.; Shimizu, K.; Parera, J. M. *Appl. Catal. A* **2002**, *230*, 137.
35. Landau, M. V.; Titelman, L.; Vradman, L.; Wilson, P. *Chem. Comm.* **2003**, 549.
36. Sing, K. S. W. *App. Chem.* **1982**, *54*, 2201.
37. Ward, D. A.; Ko, E. I. *J. Catal.* **1994**, *150*, 18.
38. Hara, S.; Miyayama, M. *Solid State Ionics* **2004**, *168*, 116.
39. Chang, J.-C.; Ko, A.-N. *React. Kinet. Catal. Lett.* **2004**, *83*, 283.
40. Xu, B.-Q.; Sachtler, W. M. H. *J. Catal.* **1997**, *167*, 224.
41. Signoretto, M.; Melada, S.; Pinna, F.; Polizzi, S.; Cerrato, G.; Mortera, C. *Micro. Meso. Mater.* **2005**, *81*, 19.
42. Ai, M. *J. Catal.* **1975**, *40*, 327.
43. Aramendia, M. A.; Borau, V.; Jimenez, C.; Marinas, J. M.; Porras, A.; Urbano, F. *J. Catal.* **1996**, *161*, 829.
44. Cho, Y.-G.; Ko, A.-N. *J. Chin. Chem. Soc.* **2000**, *47*, 1205.
45. Dalai, A. K.; Das, D.; Mishra, H. K.; Parida, K. M. *J. Mol. Catal. A* **2002**, *189*, 271.
46. Parida, K. M.; Samantaray, S. K.; Mishra, H. K. *J. Colloid Interf. Sci.* **1999**, *216*, 217.
47. Makarova, M. A.; Paukshtis, E. A.; Thomas, J. M.; Zamaraev, K. I. *J. Catal.* **1994**, *149*, 36.